Automotive Thermoelectric Generator impact on the efficiency of a drive system with a combustion engine

Andrzej Ziolkowski[1,*]

[1]Poznan University of Technology, Faculty of Working Machines and Transportation, ul. Piotrowo 3, 60-965 Poznan, Poland

Abstract. Increasing the combustion engine drive systems efficiency is currently being achieved by structural changes in internal combustion engines and its equipment, which are geared towards limiting mechanical, thermal and outlet losses. For this reason, downsizing. In addition to these changes, all manner of exhaust gas energy recovery systems are being investigated and implemented, including turbocompound, turbogenerators and thermoelectric generators. The article presents the author's idea of a thermoelectric generator system of automotive applications ATEG (Automotive Thermoelectric Generator) and the study of the recovery of exhaust gas energy stream. The ATEG consists of a heat exchanger, thermoelectric modules and a cooling system. In this solution, 24 commercial thermoelectric modules based on Bi_2Te_3 (bismuth telluride) were used. Measurements were made at two engine test sites on which SI and CI engines were installed. The exhaust gas parameters (temperature and mass flow rate), fuel consumption and operating parameters of the ATEG – the intensity and the voltage generated by the thermoelectric modules and the temperature on the walls of the heat exchanger – were all measured in the experiments. Based on the obtained results, the exhaust gas energy flow and the power of the ATEG were determined as well as its effect on the diesel engine drive system efficiency.

1 Introduction

According to the sustainable development policy implemented within the framework of the Europe 2020 strategy it is necessary to reduce the consumption of conventional energy sources (oil, gas and coal) in order to build a competitive low-carbon economy. This policy is implemented by a number of legal norms that imply limiting emissions of GHG (greenhouse gases) especially CO_2 [1-4].

In 2007, the EC (European Commission) proposed a 30% reduction of greenhouse gas emissions in developed countries by the year 2020, and suggested that the European Union itself should make a firm independent commitment to achieve at least a 20% reduction in greenhouse gas emissions [5-6]. For the automotive industry road emissions standards were introduced for either CO_2 emission or fuel consumption [7-9]. According to Arena, et al. [10], CO_2 emissions from road transport sector constitutes 16.4% of global emissions. Powering vehicles is currently responsible for 38% of the annual global demand for oil. Road transport is also responsible for emissions of CO, HC, NO_x, PM [11-14].

Most of the chemical energy contained in the fuel is drained through both the cooling system, as well as in the form of heat and pressure in exhaust gases [15]. There is a large potential for heat energy recovery from exhaust gases, as its share in the energy balance for SI engines can constitute as much as 45%. For CI engines, it is assumed that the share of thermal energy loss in the exhaust gas is a maximum of 35% [16]. For this reason, systems are developed and implemented that work in the Clausius-Rankine cycle as well as thermoelectric generators for automotive applications ATEG [17-21]. At a conference organized by German Institute of Automotive Engineering IAV in 2014, Iriyama [22] the representative of Toyota Motor Corporation, presented the company's strategy for reduction of fuel consumption in order to comply with the increasingly stringent CO_2 emission limits. The strategy is based on reducing the heat loss in vehicles – primarily through the use of automotive thermoelectric generators (ATEG). A prototype TEGS (Thermoelectric Generation System) based on an ATEG was presented. Cleary et al. [23] presented two prototypes of ATEGs dedicated to passenger vehicle and heavy-duty vehicle (HDV) engines. In the first case, the ATEG was presented with a power rating of 200 W dedicated to Honda Accord fitted with an SI engine. The second generator was dedicated to a tracked combat vehicle (Bradley) used mainly by the US army. In addition to the above solutions, prototypes developed by international research and development centers have been presented in literature [24-29]. The determining factor in the development of ATEGs is to develop thermoelectric materials with a higher ZT index. Intense research is therefore carried out to implement thermoelectric modules based on materials for mass production capable of generating greater power [30-33] and working within a broader temperature range compared to conventional Bi_2Te_3 based applications.

* Corresponding author: andrzej.j.ziolkowski@put.poznan.pl

2 Characteristic of ATEG generator

ATEG is a modular generator and it consists of three main elements: a heat exchanger, commercial thermoelectric modules and cooling elements (Fig. 1, Tab. 1). The main part of the heat exchanger, onto which thermoelectric modules are arranged has a rectangular shape. Its width is almost twice its height. In order to ensure a uniform temperature distribution along the heat exchanger a ribbing of increasing cross-section was mounted inside. It was calculated that four modules would be arranged longitudinally on each side of the heat exchanger. There were two rows of modules on the top and bottom sides of the heat exchanger and one row on each side. This gives a total of 24 modules. There was one dedicated cooling panel for each row of modules, which was attached to the heat exchanger by the means of a screw connection. This allowed the use of thermoelectric modules of different thickness. A special silicate thermal grease was applied between the modules and the walls of the heat exchanger, which facilitated the transfer of heat from the walls of the heat exchanger to the hot side of the module and helped reduce possible heat leaks arising from the surface roughness of the heat exchanger and other material imperfections and faults.

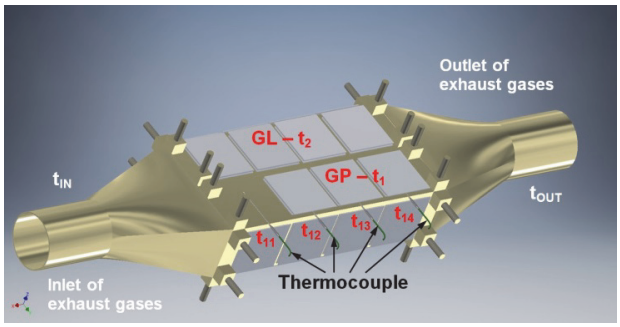

Fig. 1. View of ATEG generator.

Table 1. Characteristics of the ATEG generator.

Parameter	Value
Length	671 mm
Width	200 mm
Height	135 mm
Inlet diameter	60 mm
Material	Aluminum alloy with thickness of 2 mm
Number of modules	24
Module arrangement	Top and bottom walls – 2 rows with 4 modules each, Side walls – 1 row with 4 modules
Type of modules used	TMG-241-1.4-1.2 by Ferrotec NORD
Number of cooling panels	6
Generated nominal power	225.6 W
Generated nominal voltage without load	300 V
Generated nominal voltage with load	151.2 V

3 Research methodology

3.1 Measurement conditions in the engine test beds

Measurements of the recovery of waste energy from the exhaust gas using an ATEG were carried out on a static using a 1.2 TSI (turbo stratified injection) and on dynamic engine dynamometer using a 1.3 SDE (small diesel engine). In order to determine the engine power band for the test bed of heat recovery from exhaust gases tests were made under real operating conditions in accordance with the RDE methodology. The study selected a two vehicles equipped with a 1.2 TSI and 1.3 SDE engines, which is also located on an engine test beds (Tab. 2).

Table 2. Characteristics of the engines used for test.

Parameter	Value	
	1.2 TSI	1.3 SDE
Type of engine	Spark ignition	Compression ignition
Displacement	1.2 dm^3	1.3 dm^3
Number of cylinders	4	4
Power output	77 kW @ 5000 rpm	66 kW @ 4000 rpm
Torque	175 Nm @ 1550–4100 rpm	200 Nm @ 1750 rpm
Emissions standard	Euro 5	Euro 4
Exhaust gas aftertreatment	TWC with lambda control	DOC

In order to best mimic the registered working conditions of the first vehicle's drive unit when testing it on a static engine test bed, it was decided that the research will be carried out at three different load characteristics – constant speed value of the engine crankshaft with the load changing at 20 N·m intervals (Fig. 2 – marked with pink dots) first characteristics has been defined for 1800 rpm (six operating points), the second for 2200 rpm (five operating points) and third to 2800 rpm (five operating points). The study also included the engine idling state (800 rpm). This gives a total of 17 operating points of the engine, where the tests were carried out under laboratory conditions.

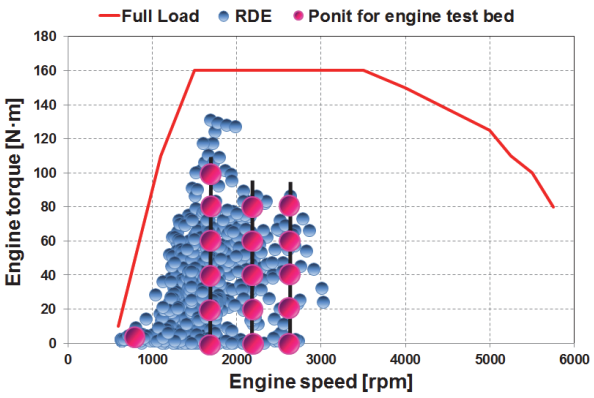

Fig. 2. Operating points for the engine of the test vehicle achieved in a test carried out in accordance with the RDE methods with its full power characteristic.

Using the Step Sequence Editor, the recorded driving profile of the vehicle expressed as a function $V = f(t)$ along with the road gradient was uploaded to the ISAC 400 software in dynamic test bed. Additionally, the vehicle speed profile was integrated with the gear ratios of the transmission in the simulation software, which was necessary for a proper operation on the test stand. A similarity of the speed profile recorded in the road test to that obtained on the test stand was observed (Fig. 3). Only in individual points of work, differences were spotted. This may result from the characteristics of the transmission and clutch operation. In the road test, the use of clutch by the driver is practically unrepeatable, while on the test stand the characteristics of the clutch and transmission operation is preset and repeatable for each gear change. This, however, does not significantly influence the difference between the average speeds in the road test and those reproduced on the test stand – they were 31.8 and 31.7 km/h respectively.

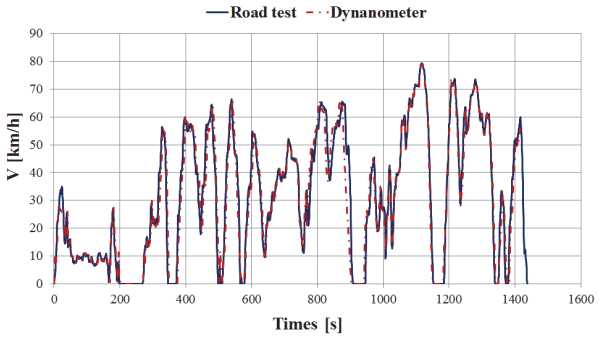

Fig. 3. Comparison of the speed profiles in the road test and on the test stand.

The fact of successful reproduction of the actual driving profile of a vehicle on an engine test bed is confirmed by the linear relation between the actual and the reproduced profiles, whose coefficient of determination is $R^2 = 0.93$ (Fig. 4). From the statistical analysis, we know that obtaining a coefficient in the range of 0.9–1.0 confirms a very good compatibility of the model with the exogenous variable.

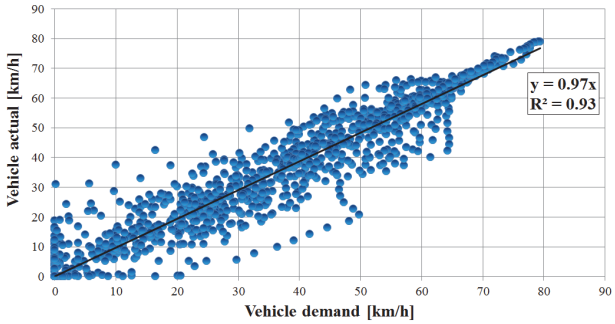

Fig. 4. Correlation of the speed in the road test and that obtained on the test stand.

During the tests of heat recovery from exhaust gases performed on a static and dynamic engine test bed the following parameters were measured:

- momentary fuel consumption G [g/s] – mass fuel gauge from Automex and AVL company,
- crankshaft rotational speed S [rpm] and engine torque T [N·m] – stationary engine test bed made by Automex company, dynamic engine test bed made by AVL company and equipped with an eddy current brake with an inductive engine speed sensor,
- exhaust mass flow rate EFM [kg/h] – with Semtech-Ecostar,
- exhaust gas temperature in measurement points [°C] – thermocouple,
- the temperature of the hot side of the thermoelectric modules [°C] (first and last module in each row) – thermocouple,
- the mass flow m_{cool}·[dm^3/h] and temperature t_{cool}· [°C] of the coolant,
- voltage U [V] and current I [A] generated by the modules – a custom-made measurement system of author design.

3.2 Equipment used for tests

The first instrument used for research was the Semtech-Ecostar. This is another device from the Setmtech® series – a successor to the Semtech DS analyzer. Example of use Semtech DS in research are presented in [34-39]. The main difference between these devices is that Semtech-Ecostar is made up of separate modules (Fig. 5):

- FEM module for measuring the concentration of CO_2, CO, HC (NDIR analyzer),
- NO_x module for the measurement of NO_x (NO and NO_2) concentration using the NDUV analyzer,
- FID module to measure THC with a FID analyzer,
- PDM module to power supply system for each component.

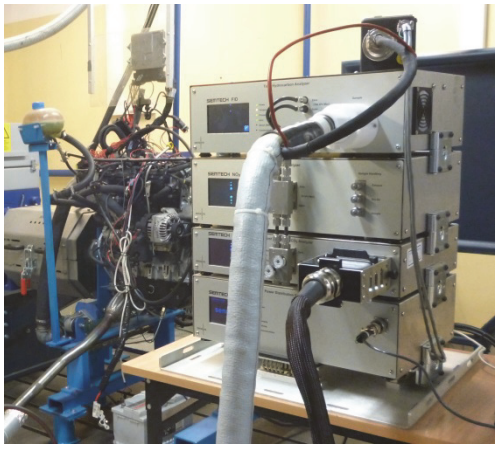

Fig. 5. Semtech-Ecostar instrument used to measure emissions in accordance with the RDE methodology.

In the case when of all the modules are used (of the gas measurement section) they must be connected together by a CAN communication wire (green lines in Fig. 6). The FEM module is connected via a special cable with a flow meter for measuring thermodynamic parameters of exhaust gases (mass flow, temperature and

pressure). This line is supplied a sample of exhaust gas that passed through the NDIR analyzer (measuring CO_2, CO and HC) is directed to the NO_x module with three connectors, wherein the measurement of NO and NO_2 takes place.

Apart from the exhaust gas sample a special conduit transmits the signal from the vehicle global positioning system (GPS) and weather sensor used to measure the atmospheric conditions (temperature, pressure, humidity), which are connected to the flow meter. A computer for system control and a signal converter from the vehicle's diagnostic system are connected using the AUX2 connector to the PDM, FEM and NO_x modules. Each module is equipped with one AUX1 and one AUX2 connection point. The signal from the power supply module for the heated wire is sent to the FID module. Semtech-Ecostar device can be powered by a PDM module, to which voltage is supplied from the grid or from the car battery. It is also possible to directly connect the modules to the mains. Due to the modular design of the instrument it can perform measurement of all gaseous compounds simultaneously, or separately using a single module.

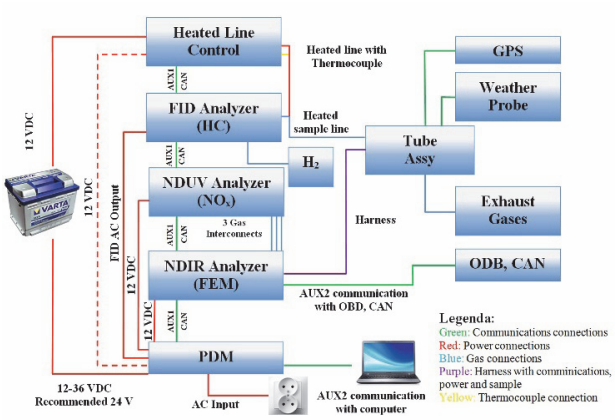

Fig. 6. Diagram of the Semtech-Ecostar system used for testing – section responsible for the measurement of gaseous compounds.

To register the temperatures and pressures two IOTECH Personal Daq/3000 signal converters were used. The measurement module was equipped with a USB interface and high-speed A/D converter (1 MHz/16 bit). The transmitter has 16 single-ended type of analog inputs (8 differential inputs), 4 analog outputs, 24 digital input/output lines, and it is possible to program the machine in 7 ranges from ±100 mV to ±10 V. Information from the sensor is transmitted to a computer which records the data of a given frequency.

The custom measurement system to measure the voltage and current generated by the modules consists of: the main module (which includes, among others a USB-600 measuring card manufactured by National Instruments having 8 analog inputs and 4 digital inputs), two converters for voltage and current measurement fitted on a PCB, a slide resistor for setting the load of the system as well as control software. The main module is supplied with a voltage of 220 V. The software allows for monitoring of the generated voltage and current in real time (in numerical and graphic form) as well as data recording with a frequency of 1 Hz. It uses algorithms to calculate the generated power in Watts and the energy expressed in kWh. A measuring device records the total value of the voltage and current of all modules, but also has the ability to measure these values for individual modules.

3.3 Method for placing ATEG generator in the exhaust system of engines tested

Both test stands were equipped with complete exhaust systems such as those used in motor vehicles. In order to indicate the location of the ATEG in the system a set of preliminary measurements of the exhaust gases thermodynamic parameters were carried out as according to the diagrams in Fig. 7–8.

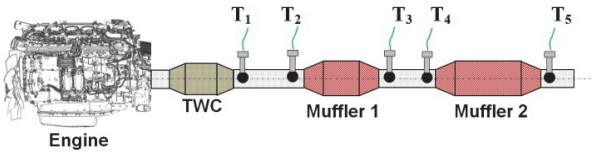

Fig. 7. The distribution of temperature and pressure measurement points in the 1.2 TSI engine exhaust system.

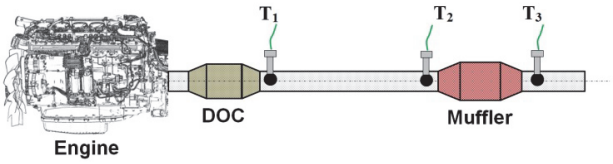

Fig. 8. The distribution of temperature and pressure measurement points in the 1.3 SDE engine exhaust system.

At all points of the 1.2 TSI engine operation constant temperature characteristics have obtained in the exhaust system. Therefore, not all research results have been presented. On the first engine characteristics at $S = 1800$ rpm and $T = 60$ N·m, the highest exhaust gas temperature was recorded after the TWC catalytic reactor, which was $T_1 = 580.1$ °C. The resulting temperature characteristics were used to determine the location of the ATEG in the 1.2 TSI engine exhaust system. From the initial tests, locating the generator directly behind the TWC catalytic reactor was excluded as a possibility, because in most of the analyzed engine operating points the exhaust gas temperature in that area exceeded 600 °C. This was mainly related to loads over 40 N·m. The design assumptions are that the exhaust gas temperature at the entrance to the ATEG will not exceed 500 °C. This was related both to the materials used for the heat exchanger construction as well as to the maximum operating temperature of the hot side of the used TEM modules. The second potential solution was to locate the energy recovery system at the first muffler location. But this was only possible for a limited engine operating range. For this reason, it was decided that the ATEG in the energy recovery study of the waste energy stream would

be placed at a position slightly away from the second muffler (Fig. 9). It has also been assumed that the first muffler will be removed from the exhaust system because it causes a significant drop in exhaust gas temperature (40–80 °C).

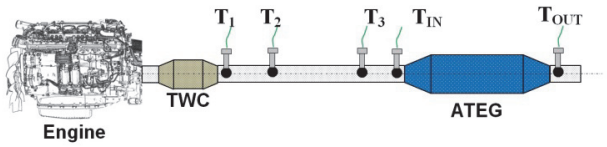

Fig. 9. Distribution of temperature measurement points in the 1.2 TSI engine exhaust system, with the ATEG.

For the 1.3 SDE engine, the exhaust gas temperature was relatively low, which resulted in the placement of the generator directly behind the catalytic converter DOC (Fig. 10).

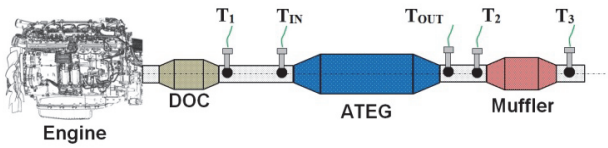

Fig. 10. Distribution of temperature measurement points in the 1.3 SDE engine exhaust system, with the ATEG.

4 Energy balance of engine exhaust system with ATEG

4.1 Energy balance of engine 1.2 TSI and 1.3 SDE engine

The choice of the 1.2 TSI engine operating points for the analysis was primarily related to the steady-state temperature characteristics, as was the case for measurements made for the exhaust system without the ATEG. Primarily, it was shown that the exhaust gas temperature was significantly reduced in the muffler. This was confirmed by the recorded temperature characteristics at points T_2 and T_3 for the considered operating area of the combustion engine. When a muffler was installed in the exhaust system, the temperature difference between T_2 and T_3 ranged between 40–80 °C. Removing the muffler resulted in a decrease in that range. For individual engine load characteristics at $T = 60$ N·m it reached a value of:

- $S = 1800$ rpm: $T_2 - T_3 = 17.5$ °C,
- $S = 2200$ rpm: $T_2 - T_3 = 10.7$ °C,
- $S = 2600$ rpm: $T_2 - T_3 = 6.2$ °C.

The exhaust gas temperature at the entrance of the ATEG was similar to that recorded before the second muffler. For $S = 1800$ rpm and $T = 60$ N·m it was 390 °C (Fig. 11).

For the measurements performed on the dynamic engine test bed with the 1.3 SDE, the temperature at point 1, behind the diesel oxidation catalyst, did not exceed 250 °C (Fig. 12). At the entry to the ATEG it reached a maximum of 200 °C. It was also observed that the measured temperature increased with time. This was related to the thermal stabilization of the exhaust system, which was reached after 400 s of operation. The maximum temperature drop in both the ATEG and the muffler was 53 and 31 °C.

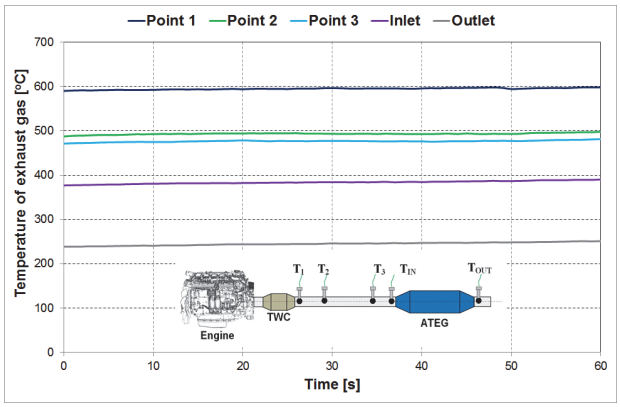

Fig. 11. The exhaust system temperature of a 1.2 TSI engine equipped with an ATEG on a static engine test bed.

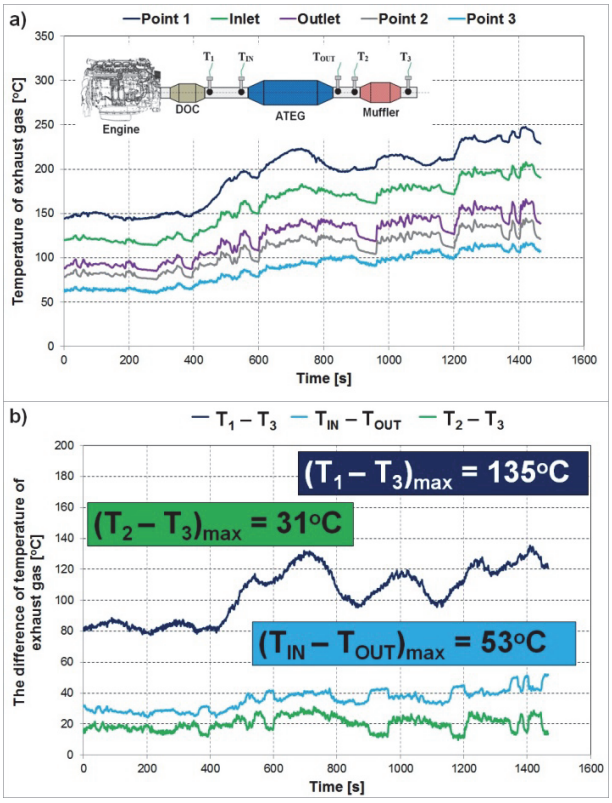

Fig. 12. The exhaust system temperature of a 1.3 SDE engine equipped with an ATEG on a dynamic engine test bed in an actual vehicle driving cycle: a) at points T_1–T_3 and T_{IN}–T_{OUT}, b) differences $T_1 - T_3$, $T_{IN} - T_{OUT}$ and $T_2 - T_3$.

4.2 The temperature distribution on the walls of the ATEG

An important factor influencing the obtained ATEG power was the temperature distribution on its walls. Due to the nature of the TEM modules operation the distribution must be practically uniform on each of them. The developed design uses 24 commercial TEM units,

which are combined in series into a single system. In this combination, the current flows through all the elements, maintaining a constant value of intensity I, while the electrical voltage U is additive. In the case of TEM modules its value is closely linked to the temperature difference between the hot and the cold side. If temperature differences occur between the individual TEM modules when connected in series, the total value of the voltage and current that the system generates will change. This will translate into power generated by the ATEG. Therefore, the temperature distribution on the individual walls of the ATEG during the tests was presented. The generator consists of four walls, which for the purposes of this analysis have been indicated as: top, bottom, left and right walls. The top and bottom walls provided two rows of four TEM modules, while the lateral (left and right) walls one row each. One sensor for measuring the temperature was placed on each hot side. Temperature measurement points on the ATEG walls were defined in the following manner (Fig. 13):

- upper right wall UR – T_{11}, T_{12}, T_{13}, T_{14},
- upper left wall UL – T_{21}, T_{22}, T_{23}, T_{24},
- right wall R – T_{31}, T_{32}, T_{33}, T_{34},
- left wall L – T_{41}, T_{42}, T_{43}, T_{44},
- lower right wall LR – T_{51}, T_{52}, T_{53}, T_{54},
- lower left wall LL – T_{61}, T_{62}, T_{63}, T_{64}.

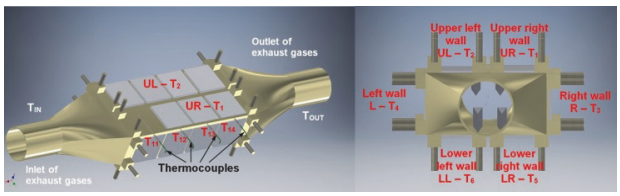

Fig. 13. Location of temperature measuring points on the walls of the ATEG.

Temperature in ATEG was measured in 24 points. The analysis of the results revealed that the temperature differences between the various modules were not significant, and demonstrated a linear relationship. Therefore, only the data for the first and last TEM unit in the row will be presented.

The test driving cycle performed on a dynamic engine dynamometer with the 1.3 SDE similar temperature distributions on each wall were obtained. The study was carried out for a thermally stable engine – the coolant temperature was 90 °C. The engine was heated up before each measurement, and then left for the temperature of the exchangers walls to stabilize. The temperature difference between the first and the last TEM module on each panel was calculated for the mean value obtained throughout the test cycle:

- $\Delta T_1 = T_{14} - T_{11}$,
- $\Delta T_2 = T_{24} - T_{21}$,
- $\Delta T_3 = T_{34} - T_{31}$,
- $\Delta T_4 = T_{44} - T_{41}$,
- $\Delta T_5 = T_{54} - T_{51}$,
- $\Delta T_6 = T_{64} - T_{61}$.

On the top and bottom walls of the heat exchanger the biggest drop in temperature was recorded for ΔT_1, which was 4.9 °C and ΔT_2 = 4.9 °C (Fig. 14a). On the side walls the differences were slightly lower ΔT_3 = = 4.5 °C and ΔT_4 = 4.6 °C (Fig. 14b). Recorded temperature distributions on the walls of the heat exchanger resulted in the obtained values of voltage and current generated by the TEM modules in a given row. Comparing the temperatures of the upper and lower walls to the side walls resulted in greater differences than the change registered between the far modules in a row.

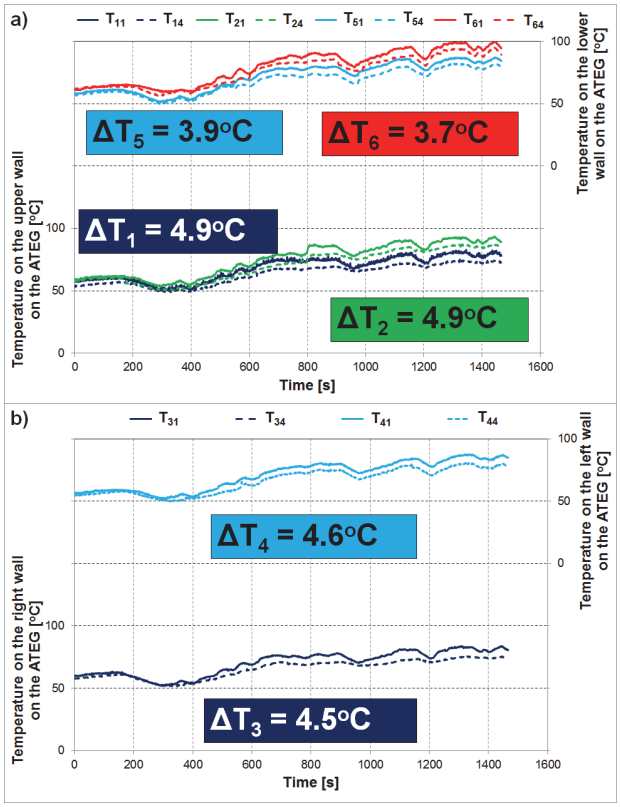

Fig. 14. The temperature distribution in ATEG mounted in the exhaust system of the 1.3 SDE in an actual vehicle driving cycle: a) the upper and lower walls, b) the side walls.

5 Efficiency of the waste energy recovery – ATEG efficiency mounted in the exhaust system of a 1.3 SDE engine

Commercial, Bi_2Te_3 based TEM units have energy conversion efficiencies not exceeding 3%. For the purpose of the research, commercial TMG-241-1.4-1.2 modules made by Ferrotec NORD were used with a power of 9.4 W each, for a total of 225.6 W. In order to determine the ATEG exhaust gas energy recovery potential, the efficiency of waste energy recovery (tantamount to ATEG efficiency) was defined, which was expressed as the ratio of power generated by the TEM modules to the amount of energy present in the exhaust gas heat exchanger fitted with the ATEG:

$$\eta_{ATEG} = \frac{P_{ATEG}}{Q_{EX}} = \frac{P_{ATEG}}{\dot{m}_{EX} \cdot c_p \cdot (T_{EX} - T_A)} \quad (1)$$

where: η_{ATEG} – ATEG efficiency [–],
P_{ATEG} – power generated by the TEM modules [kW],
Q_{EX} – energy rate in the exhaust gas [kW],
$\dot{m}_{EX}$ – exhaust mass flow rate [kg/s],
T_{EX} – temperature of exhaust gas [°C],
T_A – temperature of ambient air [°C].

The power of the TEM module is determined based on the voltage and current recorded by the developed measurement system. The amount of energy in the exhaust gas is calculated using equation (1). The exhaust gas temperature T_{EX} is construed as the average ATEG temperature:

$$T_{EX} = \frac{T_{IN} - T_{OUT}}{2} \tag{2}$$

where:
T_{EX} – average temperature inside the ATEG [°C],
T_{IN} – temperature at the inlet to the ATEG [°C],
T_{OUT} – temperature at the outlet from ATEG [°C].

In the measurements carried out on the 1.3 SDE engine on a dynamic test stand, relatively low values of power generated by the ATEG were achieved. Therefore, only the waste heat recovery efficiency for the module coolant temperature of $T_{cooling}$ = 10°C was presented (Fig. 15). The highest value occurred at deceleration (simulated vehicle braking) and zero acceleration (vehicle stationary). This was mainly due to the advantage of a constant exhaust gas mass flow resulting in a uniform temperature distribution on the walls of the heat exchanger and the ATEG. This reduced the pressure pulsations in the engine exhaust system. With the increasing speed (acceleration of the vehicle) there was a cyclical decline in the waste energy recovery efficiency due to sudden changes in the exhaust gas thermodynamic parameters. The key, in this case, was the relatively low temperature of the exhaust gas – the value on the walls of the heat exchanger did not exceed 100 °C in the tests.

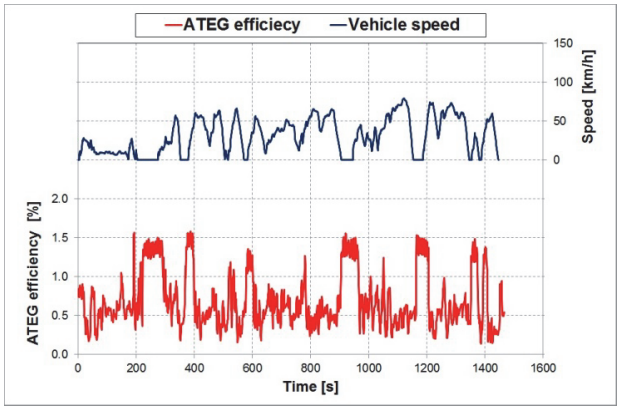

Fig. 15. The efficiency of the ATEG fitted in the exhaust system of a 1.3 SDE engine in an actual vehicle driving cycle.

In addition to determining the ATEG efficiency, it is also important to determine the potential exhaust gas energy recovery (waste energy) that is transferred to the heat exchanger walls. In this case, the temperature drop ΔT_{ATEG} plays a key role. Some of the designated waste energy is lost on the walls of the diffuser and the confusor of the heat exchanger as well as following the internal flow resistance. For this analysis, it was assumed that it equaled half of the total ATEG calculated exhaust gas energy flow. In the test driving cycle, the average value of the exhaust gas energy flow in the ATEG was Q_{EX} = 0.67 kW, and reached a maximum of 4.05 kW (Fig. 16).

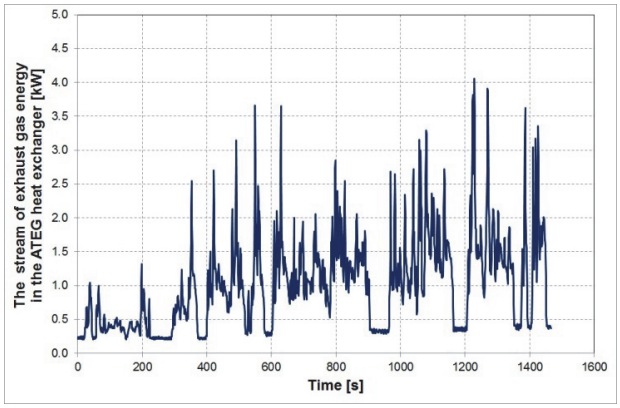

Fig. 16. The exhaust gas energy flow in the ATEG heat exchanger mounted in the exhaust system of a 1.3 SDE engine in an actual vehicle driving cycle.

6 Drive system efficiency with the 1.2 TSI and 1.3 SDE engine including the ATEG

The overall efficiency of an internal combustion engine is a measure of the use of energy contained in the fuel. This provides a view of the efficiency of conversion of the heat energy contained in the fuel into mechanical energy of the engine. This efficiency is also considered the inverse of specific fuel consumption and can be expressed as:

$$\eta_o = \frac{P_e}{G \cdot GCV} = \frac{1}{BSFC \cdot GCV} \tag{3}$$

where:
η_o – overall engine efficiency,
P_e – engine power output,
G – second-by-second fuel consumption,
GCV – gross calorific value,
BSFC – brake specific fuel consumption.

In order to determine the efficiency of a drive system η_{DSE} fitted with an ATEG, formula (3) should be used taking into consideration the power generated by the generator P_{ATEG}. Adding the ATEG power P_{ATEG} (using the values of voltage and current obtained using the developed measurement system) to the output of the engine P_e is justified, because the generator produces electrical power from the exhaust gas energy, which, in internal combustion engines, is treated as a loss (failure to use this waste energy generated by the combustion of the air-fuel mixture). This increases the efficiency of the drive system because the engine produces a greater amount of energy with the same amount of fuel. The thermal energy loss of the exhaust gas is also limited. In order to determine the increase of the powertrain

efficiency through the application of an ATEG in the exhaust system, the overall efficiency of the engine η_o must be deducted from the efficiency of the powertrain η_{DSE} (4).

$$\Delta\eta_{DSE} = \eta_{DSE} - \eta_o = \frac{(U \cdot I)_{ATEG}}{G \cdot GCV} \quad (4)$$

where:
η_{DSE}– the efficiency of the drive system including the ATEG,
U_{ATEG} – voltage generated by the TEM modules,
I_{ATEG} – current generated by the TEM modules.

Brake specific fuel consumption in the studies conducted for 1.2 TSI engine was in the range of 261.3–482.5 g/kWh (Tab. 3). The smallest value indicates the greatest overall efficiency of the engine, which was recorded for S = 2600 rpm and loads of 80 N·m. It amounted to 32.8% efficiency respectively. For S = 1800 rpm and T = 100 Nm overall efficiency was 29.4% and for S = 2200 rpm and T = 80 N·m amounted to 32.3%. For idling (the lowest possible speed of the crankshaft without load) and neutral (increased speed of the crankshaft without load) BSFC and efficiency are not calculated, because the engine does not generate any power output that would be transmitted to the receiver. It only generates power as needed to overcome the resistance of its operation. Due to the existence of these points in real road driving conditions a decision was made to also include these points in the analysis. In these cases, only the value of power generated by ATEG will be presented without determining its effect on the overall efficiency of the engine.

Table 3. Comparison of specific fuel consumption and overall efficiency of the tested engine.

Engine speed [rpm]	Torque [N·m]	BSFC [g/kWh]	Efficiency [%]
900	0	–	–
1800	0	–	–
	20	482.5	17.8
	40	370.2	23.1
	60	324.8	26.3
	80	293.2	29.2
	100	291.4	29.4
2200	0	–	–
	20	476.8	18.0
	40	345.9	24.8
	60	286.6	29.9
	80	265.1	32.3
2600	0	–	–
	20	492.7	17.4
	40	367.9	23.2
	60	267.9	31.2
	80	261.3	32.8

In all load characteristics for 1.2 TSI engine a trend of increased ATEG power generation with increasing engine torque (Fig. 17) could be observed. This is logical, because at higher loads the engine produces more exhaust gases at a higher temperature. The highest values of P_{ATEG} were as follows:

- 1800 rpm – 90.1 W,
- 2200 rpm – 98.8 W,
- 2600 rpm – 189.3 W.

For idling of the engine (S = 900 rpm & T = 0) P_{ATEG} did not exceed 1 W. The obtained test results did not reach the ATEG nominal power, which is equal to 225.6 W. The system generated at most 84% of its maximum nominal power.

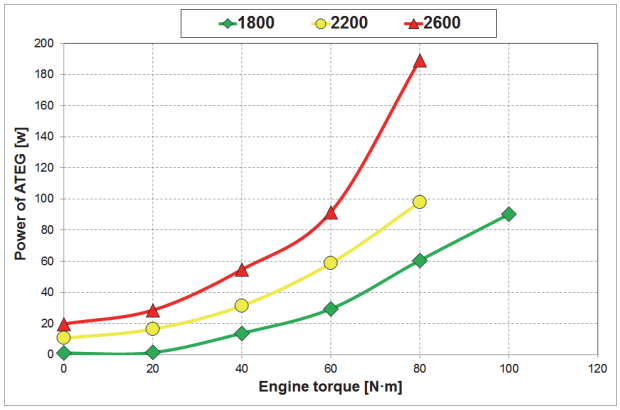

Fig. 17. The calculated power generated by the thermoelectric generator modules (ATEG) during tests.

The efficiency of the drive system including, the energy generated by the ATEG was determined using equation (4) for both engines. According to this assessment, the largest growth of efficiency of the drive system with 1.2 TSI engine was obtained for S = 2600 rpm (Fig. 18. The energy generated by the ATEG over the tested range of engine operation does not constitute a significant share of the total energy. This was mainly the result of the failure to achieve the nominal power of the generator. The above analysis has not taken into account the power loss occurring in the ATEG associated with resistance to the flow of exhaust gases.

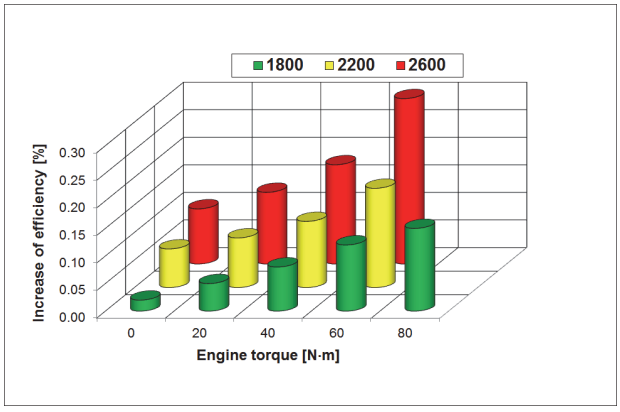

Fig. 18. Increase in overall efficiency of the test engine, through the application of ATEG in the exhaust system.

The increase in the efficiency of the drive system fitted with the 1.3 SDE engine by utilizing the power generated by the ATEG did not exceed 0.27% (Fig. 19)

and the average value throughout the experiment was 0.06%. This was mainly due to the low exhaust gas temperature, which was a consequence of low energy consumption in the test driving cycle. The greatest increase in the value of powertrain efficiency was recorded at maximum torque, which was reflected in the temperature of the exhaust gas – the efficiency was the highest in these operating points. These, however, were only single points recorded in the measurement during high accelerations.

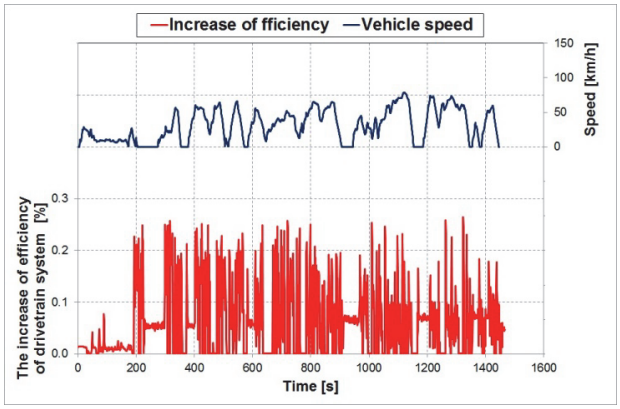

Fig. 19. The increase in the efficiency of the drive system fitted with the 1.3 SDE engine including the ATEG in an actual vehicle driving cycle.

7 Conclusion

The paper presents a study of the impact of a developed ATEG prototype the efficiency of the drive system fitted with the modern spark ignition engine designed in accordance with the principles of downsizing and compression ignition engine. These studies were performed on a static and dynamic engine test bed. In order to determine the engine power band and vehicle speed profile for the test bed of heat recovery from exhaust gases tests were made under real operating conditions in accordance with the RDE methodology.

The developed design of the ATEG was characterized by a nearly uniform distribution of temperature on each row of the TEM modules. The greatest differences of temperature between the first and the last module did not exceed 5 °C. The temperature differences among the walls were slightly higher. Such a distribution of temperatures results in similar values of voltage and current generated by the TEM modules. The study also determined the exhaust gas energy recovery potential in the ATEG heat exchanger. The average value of waste energy for 1.3 SDE engine, taking into account the loss, was 0.67 kW and the maximum was 4.05 kW. The efficiency of the ATEG varied in the range of 0.14–1.6%. The increase in the efficiency of the drive system fitted with the 1.2 TSI engine by utilizing the power generated by the ATEG did not exceed 0.29%. For 1.3 SDE this value did not exceed 0.27%. In further works, aimed at improving the efficiency of the ATEG, a change in the ribs of the internal heat exchanger is planned in order to improve the transfer of the energy flow from the exhaust gas to the generator walls.

The research was funded by the National Centre for Research and Development (Narodowe Centrum Badań i Rozwoju) – research project within the Applied Research Programme (contract No. PBS3/A6/25/2015).

References

1. Z. Juda, M. Noga, *IOP Conference Series – Materials Science and Engineering* **148**, UNSP 012042 (2016), DOI: 10.1088/1757-899X/148/1/012042
2. Z. Korczewski, J. Rudnicki, *Computational Methods in Marine Engineering VI*, 490-501 (2015)
3. J. Kromulski, T. Pawlowski, J. Szczepaniak, W. Tanas, A. Wojtyla, M. Szymanek, J. Tanas, W. Izdebski, Annals of Agricultural and Environmental Medicine **23**, 373-376 (2016), DOI: 10.5604/12321966.1203908
4. J. Szczepaniak, T. Pawlowski, R. Grzechowiak, J. Kromulski, J. Rutkowski, Applied Engineering in Agriculture **31**, 709-716 (2015)
5. M. Andrzejewski, A. Merkisz-Guranowska, Journal of KONES Powertrain and Transport **22**, 257-261 (2015)
6. J. Merkisz, M. Andrzejewski, P. Fuc, P Lijewski, Journal Acta Naturalis Scientia **1**, 11-16 (2014)
7. M. Bajerlein, L. Rymaniak, Experimental and Applied Mechanics **518**, 96-101 (2014), DOI: 10.4028/www.scientific.net/AMM.518.96
8. P. Lijewski, J. Merkisz, P. Fuc, Croatian Journal of Forest Engineering **34**, 113-122 (2013)
9. P. Lijewski, J. Merkisz, P. Fuc, M. Kozak, L. Rymaniak, Applied Mechanics and Materials **390**, 313-319 (2013), DOI: 10.4028/www.scientific.net/AMM.390.313
10. F. Arena, L. Mezzana, A. Doyon, H. Suzuki, et al., Arthur D. Little (2014)
11. J. Nowakowski, K. Brzozowski, T. Knefel, *Transport Means – Proceedings of the International Conference* 333-336 (2015)
12. J. Merkisz, M. Bajerlein, P. Daszkiewicz, *Lecture Notes in Information Technology* **13**, 106-113 (2012)
13. J. Merkisz, P. Lijewski, P. Fuc, S. Weymann, Applied Engineering in Agriculture **31**, 875-879 (2015), DOI: 10.13031/aea.31.11225
14. J. Merkisz, J. Pielecha, P. Lijewski, A. Merkisz-Guranowska, M. Nowak, *WIT Transactions on Ecology and the Environment* **174**, 27-38 (2013), DOI: 10.2495/AIR130031
15. A. Elalem, M.S. El-Bourawi, International Journal of Material Forming **3**, 663-666 (2010), DOI: 10.1007/s12289-010-0857-2
16. K. Brzozowski, J. Nowakowski, Eksploatacja i Niezawodnosc – Maintenance and Reliability **16**, 407-414 (2014)

17. P. Bombarda, C.M. Invernizzi, C. Pietra, Applied Thermal Engineering **30**, 212-219 (2010), DOI: 10.1016/j.applthermaleng.2009.08.006
18. J. Dong, Y.J. Wang, R. Zhang, B. Wang, *Lecture Notes in Electrical Engineering* 139-147 (2014), DOI: 10.1007/978-3-662-45043-7_15
19. N. Esponisa, M. Lazard, L. Aixala, H. Scherrer, Journal of Electronic Materials **39**, 1447-1455 (2010), DOI: 10.1007/s11664-010-1305-2
20. S. Glover, D.L. Glover, G. Mccullough, S. Mckenna, International Journal of Automotive Technology **16**, 399-409 (2015), DOI: 10.1007/s12239-015-0041-2
21. K. Shiho, P. Soonseo, K. Sunkook, R. Seok-Ho, Journal of Electronic Materials **40**, 812-816 (2011), DOI: 10.1007/s11664-011-1580-6
22. Y. Iriyama, *4th Thermoelectric Conference Utilizing Waste Heat in Transport and Industry* (Berlin, 2014)
23. M. Cleary, Y. Zhang, A. Mazzotta, H. Young, et al., *4th Thermoelectric Conference Utilizing Waste Heat in Transport and Industry* (Berlin, 2014)
24. S. Kim, S. Park, S. Kim, S. Rhi, Journal of Electronic Materials **40**, 812-816 (2011), DOI: 10.1007/s11664-011-1580-6
25. S. Kumar, S.D. Heister, X. Xu, J.R. Salvador, et al., Journal of Electronic Material **42**, 665-674 (2013), DOI: 10.1007/s11664-013-2471-9
26. S. Kumar, S.D. Heister, X. Xu, J.R. Salvador, et al., Journal of Electronic Materials **42**, 944-955 (2013), DOI: 10.1007/s11664-013-2472-8
27. R. Kühn, O. Koeppen, J. Kitte, Journal of Electronic Materials **43**, 1521-1526 (2014), DOI: 10.1007/s11664-013-2769-7
28. D. Tatarninov, M. Koppers, G. Bastian, D. Schramm, Journal of Electronic Materials **42**, 2274-2281 (2013), DOI: 10.1007/s11664-013-2642-8
29. D. Tatarninov, D. Walling, G. Bastian, Journal of Electronic Materials **41**, 1706-1712 (2012), DOI: 10.1007/s11664-012-2040-7
30. R. Amatya, R.J. Ram, Journal of Electronic Materials **41**, 1521-1526 (2012), DOI: 10.1007/s11664-011-1839-y
31. P. Gao, I. Berkun, R.D. Schmidt, M.F. Luzenski, X. Lu, et al., Journal of Electronic Materials **43**, 1790-1803 (2014), DOI: 10.1007/s11664-013-2865-8
32. J.Y. Jang, Y.C. Tsai, Applied Thermal Engineering **51**, 677–689 (2010), DOI: 10.1016/j.applthermaleng.2012.10.024
33. K.T. Wojciechowski, M. Schmidt, R. Zybala, J. Merkisz, P. Fuc, P. Lijewski, Journal of Electronic Materials **39**, 2034-2038 (2010), DOI: 10.1007/s11664-009-1010-1
34. J. Merkisz, M. Andrzejewski, A. Merkisz-Guranowska, I. Jacyna-Gołda, Journal of KONES Powertrain and Transport **21**, 219-226 (2014)
35. J. Merkisz, M. Idzior, J. Pielecha, W. Gis, *WIT Transactions on the Built Environment* **111**, 181-189 (2010), DOI: 10.2495/UT100171
36. J. Merkisz, P. Lijewski, P. Fuc, S. Weymann, Eksploatacja i Niezawodnosc – Maintenance and Reliability **15**, 364-368 (2013)
37. J. Merkisz, J. Pielecha, *IOP Conference Series-Materials Science and Engineering* **148**, UNSP 012078 (2016), DOI: 10.1088/1757-899X/148/1/012078
38. J. Pielecha, J. Merkisz, J. Markowski, R. Jasinski, *E3S Web of Conferences* **10**, UNSP 00073 (2016), DOI: 10.1051/e3sconf/20161000073
39. J. Merkisz, J. Pielecha, W. Gis, *Proceedings of the Ninth Asia-Pacific International Symposium on Combustion and Energy Utilization* 477-482 (2008)